Synthesis of Nanoscale Mesoporous Silica Spheres with Controlled Particle Size

Robert I. Nooney,[†] Dhanasekaran Thirunavukkarasu,[‡] Yimei Chen,[§] Robert Josephs,[§] and Agnes E. Ostafin*,[†]

Department of Chemical Engineering, University of Notre Dame, Notre Dame, Indiana 46556, Radiation Laboratory, University of Notre Dame, Notre Dame IN 46556, and Department of Molecular and Cellular Biology, University of Chicago, Chicago, Illinois 60637

Received May 7, 2002. Revised Manuscript Received August 23, 2002

A simple one-step procedure is described for the synthesis of spherical mesoporous silica, in which the size of the particles is controlled over a range of diameters from 65 to 740 nm by varying the initial silicate/surfactant concentration under dilute conditions. The particles were characterized using X-ray diffraction, transmission electron microscopy, and liquid nitrogen adsorption. Synthesis using a charged template, cetyltrimethylammonium bromide, under aqueous conditions yielded particles of irregular spherical shape with highly ordered mesoporous channels. Synthesis under ethanol/water cosolvent conditions yielded smooth spheres with a starburst mesopore structure extending from the center of the particle to the circumference. All materials were thermally stable and exhibited two steps in their liquid nitrogen isotherms corresponding to reversible channel filling and non-reversible adsorption between particles. Mesopore volumes varied from 0.64 to 0.93 $cm^3\ g^{-1}$ and surface areas varied from 917 to 1373 $m^2\ g^{-1}$. From analysis of mesopore geometry and overall particle shape a three-stage mechanism for synthesis is proposed.

Introduction

There is a great deal of interest in the utilization of nanoscale particles of mesoporous silica in chromatography, surface polishing, catalysis, medical implants, and drug delivery.[1−3] Their synthesis follows a self-assembly mechanism in which physical, chemical, and structural properties of the nanoparticle are controlled by reactant ratios and experimental conditions.[4−7] For example, Cai and co-workers synthesized different particle morphologies simply by choosing sodium hydroxide over ammonium hydroxide.[8] Unger and co-workers synthesized nanoparticles using both charged and neutral templates and showed that the addition of cosolvent produced more spherical particles.[9,10] Control of nanoparticle size was recently achieved by adjusting the relative concentration of base catalyst, [11] and in a separate study it was acheived by dilution quenching and subsequent neutralization of unreacted material after very short reaction times.[12]

In the work presented here, we show an alternative method in which control of the size of spherical mesoporous nanoparticles over a wide range of diameters from 65 to 740 nm is achieved by varying the initial silicate and surfactant concentrations under dilute conditions. The result is a simple, one-step procedure for the self-assembly of highly ordered mesoporous silica nanoparticles of predetermined size. The strategies presented here may be useful in the synthesis of a wide range of metal inorganic nanocomposites for chemical sensing, materials for methane storage, quantum dot confinement, or the development of novel semiconductor devices.[13−18]

Experimental Section

Materials. Tetraethyl orthosilicate (TEOS, 99 wt %), *n*-dodecylamine (99.8 wt %), and ammonia (2.0 M NH_3 in

* To whom correspondence should be addressed. Fax: (219)-6318366. E-mail: aostafin@nd.edu.
† Department of Chemical Engineering, University of Notre Dame.
‡ Radiation Laboratory, University of Notre Dame.
§ Department of Molecular and Cellular Biology, University of Chicago.

(1) Huo, Q.; Feng, J.; Schuth, F.; Stucky, G. D. *Chem. Mater.* **1997**, *9*, 14.
(2) Ozin, G. *Adv. Mater.* **1992**, *4*, 612.
(3) Büchel, C.; Grün, M.; Unger, K. K.; Matsumoto, A: Tsutsumi, K. *Supramolecular Sci.* **1998**, *5*, 253.
(4) Monnier, A.; Schüth, F.; Huo, Q.; Kumar, D.; Margolese, D.; Maxwell, R. S.; Stucky, G. D.; Krishnamurty, M.; Petroff, P.; Firouzi, A.; Janicke, M.; Chmelka, B. F. *Science* **1993**, *261*, 1299.
(5) Firouzi, A.; Kumar, D.; Bull, L. M.; Besier, T.; Sieger, P.; Huo, Q.; Walker, S. A.; Zasadzinski, J. A.; Glinka, C.; Nicol, J.; Margolese, D.; Stucky, G. D.; Chmelka, B. F. *Science* **1995**, *267*, 1138.
(6) Huo, Q.; Margolese, D. I.; Ciesla, U.; Demuth, D. G.; Feng, P.; Gier, T. E.; Sieger, P.; Firouzi, A.; Chmelka, B. F.; Schüth, F. Stucky, G. D. *Chem. Mater.* **1994**, *6*, 1176.
(7) Anderson, M. T.; Martin, J. E.; Odinek, J. G.; Newcomer, P. P. *Chem. Mater.* **1998**, *10*, 311.
(8) Cai, Q.; Luo, Z.; Pang, W.; Fan, Y.; Chen, X.; Cui, F. *Chem. Mater.* **2001**, *13*, 258.
(9) Büchel, G.; Grün, M, Unger, K. K.; Matsumoto, A.; Tsutsumi, K. *Supramolecular Sci.* **1998**, *5*, 253.
(10) Grün, M.; Unger, K. K.; Matsumoto A.; Tsutsumi, K. *Microporous Mesoporous Mater.* **1999**, *27*, 207.
(11) Anderson, M. T.; Schulz, M. F.; Nigatu, T. G. U.S. Patent 6,-096,469, 2000.
(12) Fowler, C. E.; Khushalani, D.; Lebeau, B.; Mann, S. *Adv. Mater.* **2001**, *13*, 649.
(13) Mukherjee, P.; Patra, C. R.; Kumar, R.; Sastry, M. *PhysChemComm* **2001**, *5*, 1.
(14) Cai, W.; Zhong, H.; Zhang, L. *J. Appl. Phys.* **1998**, *83*, 1705.
(15) Aronson, B. J.; Blanford, C. F.; Stein, A. *Chem. Mater.* **1997**, *9*, 2842.
(16) Mulukurtla, R. S.; Asakura, K.; Kogure, T.; Namba, S.; Iwasawa, Y. *Phys. Chem. Chem. Phys.* **1999**, *1*, 2027.
(17) Parala, H.; Winkler, H.; Kolbe, M.; Wohlfart, A.; Fischer, R. A.; Schmechel, R.; Von Seggern, H. *Adv. Mater.* **2000**, *12*, 1050.
(18) Nooney, R. I.; Dhanasekaran, T.; Chen. Y.; Josephs, R.; Ostafin, A. E. *Adv. Mater.* **2002**, *14*, 529.

10.1021/cm0204371 CCC: $22.00
Published on Web 10/03/2002

Table 1. Molar Ratios of Reactants for Synthesis of Mesoporous Silica Nanoparticles Using Procedure 1, Heterogeneous Conditions with Charged Template

sample	H_2O	NH_3	TEOS	CTAB	particle size (nm)
A	4000	30.2	1	0.125	70
B	3000	30.2	1	0.125	120
C	2000	30.2	1	0.125	420
D	1000	30.2	1	0.125	460

Table 2. Molar Ratios of Reactants for Synthesis of Mesoporous Silica Nanoparticles Using Procedure 2, Homogeneous Conditions with Charged Template

sample	C_2H_5OH	H_2O	NH_3	TEOS	CTAB	particle size (nm)
E	500	1500	30.2	1	0.125	190
F	58	153	3.85	1	0.3	740

2-propanol) were purchased from Sigma Aldrich. Cetyltrimethylammonium bromide (CTAB, 99.8 wt %) was purchased from Calbiochem; ethanol was purchased from AAPER Alcohol and Chemical Company; and ammonium hydroxide (29 wt % NH_3 in water) was purchased from Fisher Scientific. All materials were used without further purification. Water was deionized to 18.2 MΩ cm^{-1} using an E-pure Barnstead model D4641 instrument.

Synthesis. Procedures were divided into three different groups on the basis of whether the silica dissolution time (SDT) was greater than the gelation time (GT):[7,10] (1) heterogeneous (SDT > GT) using a charged template and pure water solvent; (2) homogeneous (SDT < GT) using a charged template and water/ethanol cosolvent; and (3) homogeneous (SDT < GT) using a neutral template and water/ethanol cosolvent conditions. In all cases the sample was recovered by pressure filtration using 10 000 MWCO filter paper (Amicon), and the mesopore template was removed by calcination in air at 540 °C for 6 h.

Procedure 1: Heterogeneous Synthesis with Charged Template and Pure Water Solvent. The molar ratios of reactants using this procedure are shown in Table 1. For experiment A, the pH of 442 mL of deionized water was adjusted to approximately 11 with the addition of 10.8 g of ammonium hydroxide (29 wt % NH_3 in water). The temperature was then raised to 50 °C and 0.279 g of CTAB was added to the water with rapid stirring. The pH of the CTAB solution subsequently dropped to 10.3. The solution was allowed to cool to room temperature and 1.394 mL of TEOS was added with rapid stirring. After 2 min, the solution became slightly turbid and the pH dropped to 9.8 indicating rapid hydrolysis of the silicate was taking place. After 2 h the pH again rose to 10.6, presumably relating to silica condensation reactions. The sample was then filtered and calcined as described previously. The experiments A, B, C, and D in Table 1 were performed under identical conditions with increasing concentrations of TEOS from 1.4 to 5.3×10^{-2} M and with a constant TEOS/CTAB molar ratio of 8:1.

Procedure 2: Homogeneous Synthesis with Charged Template and Water/Ethanol Cosolvent. The molar ratios of reactants used for this procedure are shown in Table 2. For experiment E, 138 g of ethanol and 162 g of deionized water were mixed, and the solution pH was adjusted to 11.7 with the addition of 11.6 mL of ammonium hydroxide (29 wt % NH_3 in water). Following this, 0.274 g of CTAB was added with rapid stirring at room temperature. After 5 min, 1.388 mL of TEOS was added. The solution became slightly turbid 5 min later, indicating hydrolysis. The suspension was filtered after 2 h and was determined to have a final solution pH of 10.9. The second experiment labeled F in Table 2 was performed under the same conditions but a higher concentration of TEOS and CTAB was used.

Procedure 3: Homogeneous Synthesis using Neutral Template and Water/Ethanol Cosolvent. The molar ratios of reactants used to prepare samples in this procedure are shown in Table 3. For experiment G, 78.6 g of ethanol and 0.290 g of *n*-dodecylamine was added to 100 mL of deionized water with rapid stirring. The pH of the *n*-dodecylamine solution was 11.1. Next, 9.2 mL of ammonium hydroxide solution (2.0 M NH_3 in 2-propanol) was added and the solution pH increased to 11.3. After five minutes, 1.084 g of TEOS was added with rapid stirring, and after an additional 10 minutes, the solution became slightly turbid, indicating hydrolysis. The suspension was filtered after 24 h and determined to have a final pH of 10.6. The second experiment labeled H in Table 3 was performed under the same conditions with a higher concentration of TEOS and *n*-dodecylamine.

Characterization. *X-ray Diffraction.* Powder samples, of 100 mg each, were evenly dispersed onto glass slides. Patterns were collected using a Scintag XDS 2000 diffractometer with a diffractometer beam monochromator and CuKα radiation source. Scattering patterns were collected from 1.5 to 10° with a scan time of 5.0 s per 0.01° step.

Transmission Electron Microscopy. Micrographs were obtained using either a Philips CM120 electron microscope operating at 125 KV with a 35-micron objective aperture (Electron Microscopy Facility, University of Chicago) or a Hitachi H-600 operated at 80 kV with a 35-micron objective (Department of Biology, University of Notre Dame). Micrographs were recorded at a magnification of 125 000 using Kodak SO163 film that was developed in D19 for 5 min. Specimens for sectioning were embedded in LR White resin and cured prior to sectioning 70-nm thick samples. Both sectioned and as-synthesized samples were picked up on a carbon coated copper grid.

Liquid Nitrogen Isotherms. Adsorption isotherms were obtained using a Quantachrome Autosorb-1 (Chemical Engineering Department, University of Notre Dame). Powder samples of 20 mg each were outgassed to less than 5 mTorr at 200 °C for 3 h. The adsorption of liquid nitrogen was recorded using equilibration times of approximately 10 min per point. Surface area calculations were made using the Brunauer, Emmett, and Teller (BET) equation fitted to the first 10 points of each isotherm. Pore-size distributions were calculated using Schmidt's modification of the Kelvin equation to account for mono- and multi-layer adsorption.[19]

Results and Discussion

Synthesis under heterogeneous charged template conditions yielded irregular spherical particles over a wide range of particle sizes with ordered mesopores. In this work, the phrase "ordered mesopores" refers to a material that contains pores which align over long range to form a pattern observable with TEM. The respective X-ray diffraction patterns of the as-prepared samples are shown in Figure 1. In all cases (A−D), four peaks are present which can be indexed to a hexagonal unit cell. The presence of four X-ray diffraction peaks is very common in MCM-41 materials.[20] The (100) *d* spacing for all samples was greater than 4 nm and is shown in Table 4 along with cell parameters and relative intensities. The values obtained were larger than those by Cai and co-workers [8] who observed a (100) *d* spacing of 3.41 nm for particles prepared under pure water solvent conditions. The fact that long-range order is obtained by this method is quite interesting. The CTAB concentration for preparation of sample A at 1.7×10^{-3} M is significantly lower than previous concentrations used in mesoporous particle synthesis which ranged from 1.1 to 4.9×10^{-2} M.[8,10] CTAB is known to form rod-shaped

(19) Schmidt, R.; Hansen, E. W.; Stocker, M.; Akporiaye, D.; Ellestad, O. H. *J. Am. Chem. Soc.* **1995**, *117*, 4049.

(20) Beck, J. S.; Vartuli, J. C.; Roth, W. J.; Leonowicz, M. E.; Kresge, C. T.; Schmitt, K. D.; Chu, C. T−W.; Olson, D. H.; Sheppard, E. W.; McCullen, S. B.; Higgins, J. B.; Schlenker, J. L. *J. Am. Chem. Soc.* **1992**, *114*, 10834.

Table 3. Molar Ratios of Reactants for Synthesis of Mesoporous Silica Nanoparticles Using Procedure 3, Homogeneous Conditions with Neutral Template

sample	$CH_3CHOHCH_3$	C_2H_3OH	H_2O	NH_3	TEOS	n-dodecylamine	particle size (nm)
G	23.3	351	1143	3.79	1	0.29	60
H	7.76	117	381	1.26	1	0.29	550

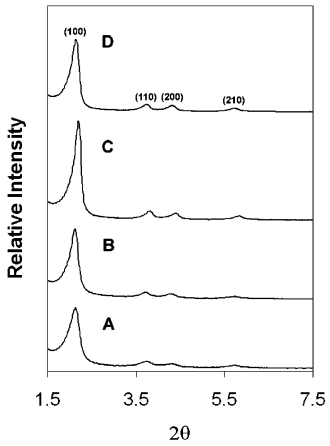

Figure 1. Powder X-ray diffraction patterns of mesoporous silica nanoparticles of samples A, B, C, and D, as-synthesized, using heterogeneous conditions with charged template, CTAB.

Table 4. Powder X-ray Diffraction Data of Mesoporous Silica Nanoparticles of Samples A, B, C, and D, As Synthesized, Using Heterogeneous Conditions with Charged Template

sample	peak	2θ	intensity	d (nm)	Å (nm)
A	100	2.13	10438	4.14	4.78
B	100	2.12	12014	4.16	4.81
C	100	2.20	16783	4.01	4.63
D	100	2.14	12390	4.12	4.76

micelles in aqueous systems above the second critical micelle concentration (CMC_2, 0.3 M) and assemble into hexagonal liquid crystals above 1.1 M.[6,21] The concentration of sample A is two orders of magnitude lower than CMC_2 for the micelle-to-rod transition under aqueous conditions and supports the argument that particle formation is silica driven.[1] The most probable reason for mesopore self-assembly is the formation of very strong multidentate linkages between silicate oligomers and the quaternary ammonium surfactant. Silica/surfactant linkages would be very stable and would also screen the repulsion interaction between adjacent micelles increasing the negative free energy for self-assembly.[1,6]

The TEM micrographs of as-prepared samples A−D (Figure 2) show that increasing the concentration of TEOS and CTAB increases the particle size from 70 to 460 nm. The top micrograph, A, shows that nanoparticles prepared at the lowest concentration of TEOS (1.4×10^{-2} M) and CTAB (1.7×10^{-3} M) in water yielded an average particle size of approximately 70 nm. The inset of micrograph A is an expanded image of a single nanoparticle in which a hexagonal array of ordered mesopores is clearly visible. The pore center-to-center distance at 4.2 nm is slightly shorter than 4.78 nm recorded from X-ray diffraction, and the difference is likely due to TEM artifact. The micrograph B shows

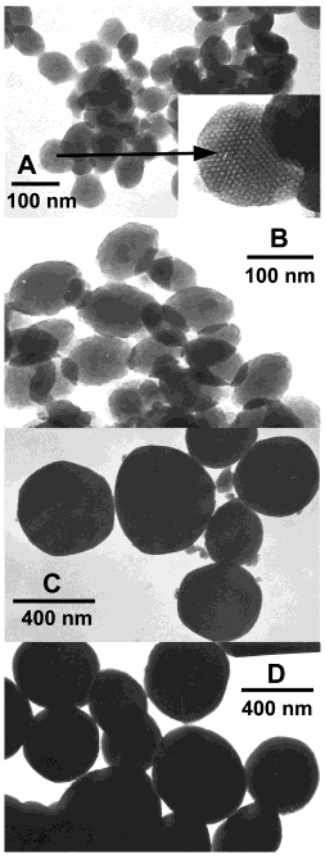

Figure 2. Transmission electron micrographs of mesoporous silica nanoparticles of samples A, B, C, and D, as-synthesized, prepared under heterogeneous conditions with charged template CTAB. The inset in micrograph A is a single nanoparticle magnified to highlight the ordered mesopore structure.

samples prepared with TEOS and CTAB concentrations of 1.9×10^{-2} and 2.3×10^{-3} M, respectively. These particles were found to be egg-shaped with an average length of 120 nm and width of 75 nm. Under heterogeneous conditions, with TEOS and CTAB concentrations of 2.3×10^{-2} and 6.2×10^{-3} M, respectively, and using NaOH as the catalyst instead of ammonia, we have also observed elongated and faceted crystals in which the greatest amount of growth occurred along the axis parallel to the direction of the pore channels.[22] On the basis of these observations, it seems likely that the preferred growth also occurred along the pore channel direction. The reason that the particles are not faceted is likely due to ammonia being used as the catalyst, which is known to lead to more spherical morphologies and is often referred to as a morphogenic catalyst.[23] Micrographs C and D obtained at higher TEOS concentrations of 2.7 and 5.3×10^{-2} M show more spherical nanoparticles with average sizes of 420 and 460 nm in

(21) Choudhary, S.; Roy Yadav, R.; Maitra, A. N.; Jain, P. C.; *Colloids Surf. A: Physiochem. Eng. Aspects* **1994**, *82*, 49.

(22) Nooney, R. I.; Dhanasekaran, T.; Chen, Y.; Josephs, R.; Meizel, D.; Ostafin, A. E. *J. Am. Chem. Soc.* **2002**, submitted for publication.

(23) Stöber, W.; Fink, A.; Bohn, E. *J. Colloid Interface Sci.* **1968**, *26*, 62.

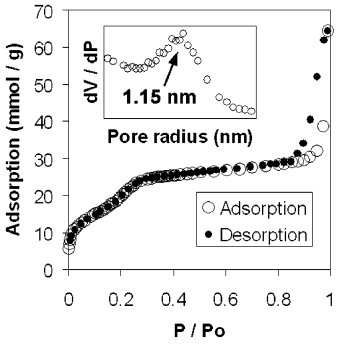

Figure 3. Liquid nitrogen adsorption isotherm of mesoporous silica nanoparticles of sample A, calcined at 540 °C for 6 h. The inset shows the pore radius distribution determined using the modified Kelvin equation.[18]

diameter, respectively. Under similar physical conditions, with approximately double the concentrations of reactants in water, Cai and co-workers observed faceted crystals larger that 1 μm in diameter, consistent with our pattern of increasing size with increasing concentration.[8]

The liquid nitrogen isotherm of sample A of this series is shown in Figure 3. The isotherm is type IV in IUPAC classification.[24] No hysteresis was observed in the desorption branch of the first step relating to capillary condensation, and this is typical of MCM-41 type materials.[19] A total mesopore volume of 0.98 $cm^3\ g^{-1}$ was recorded at 0.8 P/Po and is slightly higher than the 0.93 $cm^3\ g^{-1}$ obtained by Cai and co-workers.[8] The second step starting at 0.9 P/Po was assigned to adsorption between nanoparticles giving a total sample capacity of 2.23 $cm^3\ g^{-1}$. A small hysteresis loop in the desorption branch of the second step is probably due to pore blocking at the interface between nanoparticles. The inset of Figure 3 is a pore radius distribution graph indicating an average pore radius of 1.15 nm for these particles. For this material, a surface area of 1373 $m^2\ g^{-1}$ was obtained and is significantly higher than that recorded for conventional MCM-41 type materials at 1040 $m^2\ g^{-1}$.[20] However, care should be taken in applying these data because the onset of capillary condensation is at a very low partial pressure and may have contributed to the calculated value.

Synthesis in homogeneous conditions, using water/ethanol cosolvent and a charged template yielded smooth, spherical particles also with ordered mesopores. The X-ray diffraction patterns of the as-prepared samples E and F, in contrast to the multiple sharp peaks of the previous series, exhibit only two relatively broad peaks in each pattern (Figure 4). The larger and smaller peaks of each were indexed to the (100) and (110) diffraction planes of a hexagonal lattice. The *d* spacings for the first peaks in samples E and F were 3.66 and 3.86 nm, respectively (Table 5) and are significantly smaller than the spacings of particles prepared via the heterogeneous system. The 0.5-nm shrinkage is consistent with the 0.4 nm shrinkage of rod aggregate diameters of CTAB in water/ethanol cosolvent compared with those in H_2O alone.[25] Anderson and co-workers also observed a

(24) Sing, K. S. W. *Pure Appl. Chem.* **1985**, *57*, 603.
(25) Fontell, K.; Khan, A.; Lindstrom, B.; Maciejewska, D.; Puang-Ngern. S. *Colloid Polym. Sci.* **1991**, *269*, 727.

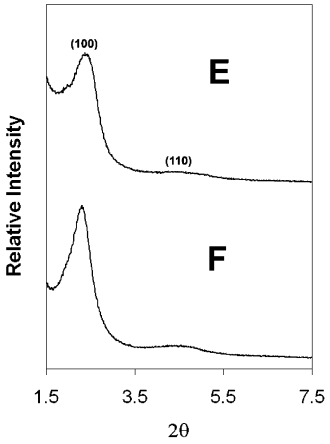

Figure 4. Powder X-ray diffraction patterns of mesoporous silica nanoparticles of samples E and F, as-synthesized, using homogeneous conditions with charged template CTAB.

Table 5. Powder X-ray Diffraction Data of Mesoporous Silica Nanoparticles of Samples E and D, As Synthesized, Using Homogeneous Conditions with Charged Template

sample	peak	2θ	intensity	*d* (nm)	Å (nm)
E	100	2.41	4469	3.66	4.23
F	100	2.29	5291	3.86	4.45

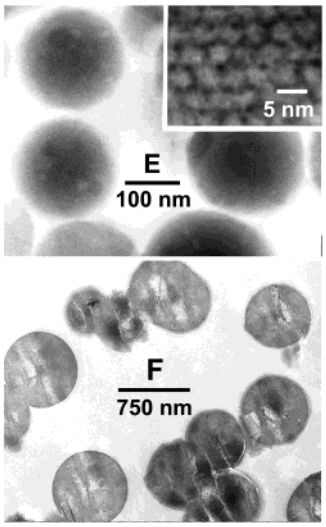

Figure 5. Transmission electron micrographs of mesoporous silica nanoparticles of samples E and F, as-synthesized, using homogeneous conditions with charged template CTAB. The inset of sample E shows an expanded section highlighting the ordered mesopore structure.

significant shrinkage in pore size of mesoporous silica when protic solvents were added.[7]

The TEM micrographs of as-prepared samples E and F (Figure 5) show that the particle size increased from 190 to 740 nm with increasing concentrations of TEOS and CTAB, indicating that particle size control with concentration is also true in cosolvent systems. The particles formed smooth spheres in the presence of a protic cosolvent in agreement with previous work by Anderson,[7] Grün, [10] and co-workers. The broader, light gray smudge marks on the nanoparticles in the micrograph of sample F in Figure 5 are artifacts of the cleaving process used in the preparation of a microtomed section. Sample E nanoparticles also formed a colloidal suspension, which was stable under quiescent conditions for several days without precipitation. Both

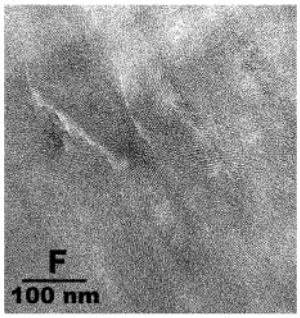

Figure 6. Transmission electron micrographs of an expanded section of sample F highlighting the ordered mesopore structure that expands out from the center in a starburst pattern.

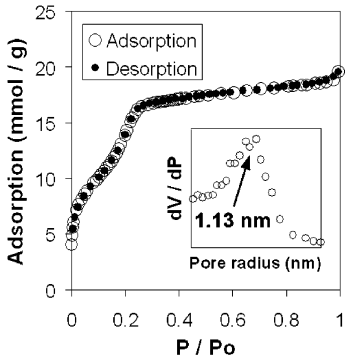

Figure 7. Liquid nitrogen adsorption isotherm of mesoporous silica nanoparticles of sample F using homogeneous conditions with charged template. The inset shows the pore radius distribution determined using the modified Kelvin equation.[18]

samples E and F could be resuspended by mild sonication in deionized water.

The inset of micrograph E in Figure 5 is an expanded image showing an ordered mesopore arrangement typical of MCM-41 materials. The pore center-to-center distance is 4.25 nm, which is 0.02 nm greater than the value obtained by X-ray diffraction. The TEM micrograph in Figure 6 is an expanded region from the middle of one nanoparticle of sample F. At the center is a regular lattice structure with a pore center-to-center distance of 4.4 nm, which is 0.1 nm smaller than that obtained from X-ray diffraction. On close inspection of the micrograph in Figure 6 we can see mesopores that expand radially from the center of the nanoparticle. In this work, only samples made using homogeneous charged template conditions yielded this starburst mesopore structure. The starburst mesopores in our work extend from the center of the nanoparticle to the circumference with a low frequency of defects in silicate deposition, suggesting a seeded growth mechanism. It should be noted that under heterogeneous conditions with a low concentration of TEOS, Cai and co-workers synthesized an agglomerated mesoporous material with a similar starburst mesopore structure and assigned this to an agglomeration of rod-shaped micelles.[8]

The liquid nitrogen adsorption isotherm of sample F is shown in Figure 7. The isotherm is also type IV in IUPAC classification, and as before, no hysteresis was observed in the desorption branch of the first step. The adsorption capacity at 0.9 P/Po is 0.64 $cm^3\ g^{-1}$ and is slightly lower that that recorded by Grün and co-workers at 0.8 $cm^3\ g^{-1}$. [10] A small, second step at 9.5 P/Po, with slight hysteresis, was assigned to adsorption

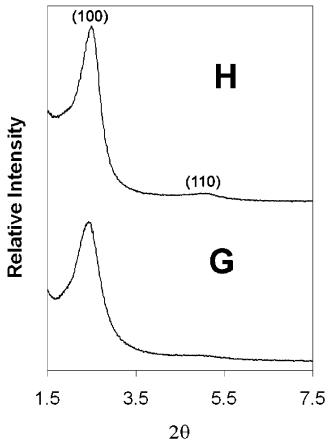

Figure 8. Powder X-ray diffraction patterns of mesoporous silica nanoparticles of samples G and H, as-synthesized, using homogeneous conditions with neutral template, *n*-dodecylamine.

Table 6. Powder X-ray Diffraction Data of Mesoporous Silica Nanoparticles of Samples G and H, As Synthesized, Using Homogeneous Conditions with Neutral Template, *n*-Dodecylamine

sample	peak	2θ	intensity	*d* (nm)	Å (nm)
G	100	2.44	6528	3.62	4.18
H	100	2.5	8077	3.53	4.08

between particles. A surface area of 917 $m^2\ g^{-1}$ at STP was calculated and is comparable to the 1100 $m^2\ g^{-1}$ recorded by Grün and co-workers.[10] The inset of Figure 7 is a pore radius distribution graph indicating an average pore radius of 1.13 nm.

In contrast to the highly ordered structures of the previous two systems, synthesis using homogeneous neutral template conditions yielded smooth spherical particles with disordered mesopores throughout. Here, the phrase "disordered mesopores" means that the material contains pores that are clearly visible using TEM but are randomly aligned in the particle. X-ray diffraction patterns of as-prepared samples G and H were similar to those obtained via the homogeneous system and showed a larger and smaller broad peak in each case (Figure 8). The two peaks of each pattern were indexed to the (100) and (110) diffraction planes of a hexagonal lattice, and the parameters obtained are given in Table 6. The *d* spacing of the first peaks in G and H were 3.62 and 3.53 nm, respectively. These values are smaller than the *d* spacings obtained from experiments A−D performed using CTAB. The origin of this decrease is difficult to determine but may be related to the fact that the template *n*-dodecylamine has a shorter carbon chain length than CTAB and interacts with silica via hydrogen bonding as opposed to electrostatic forces.[26]

The TEM micrographs of as-prepared samples G and H are shown in Figure 9. The average particle diameters obtained were 60 and 550 nm for the lower and higher concentrations of TEOS and *n*-dodecylamine, respectively. The smaller particles formed a colloidal suspension, which was stable for several days under quiescent conditions. After settling, both samples could be resuspended by sonication in deionized water. The larger particles were the most monodispersed in size obtained

(26) Auvray, A.; Petipas, C.; Anthore, R.; Rico, I.; Lattes, A. *J. Phys. Chem.* **1989**, *93*, 7458.

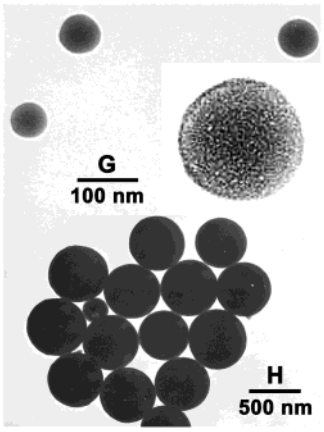

Figure 9. Transmission electron micrographs of mesoporous silica nanoparticles of samples G and H, as-synthesized, using homogeneous conditions with neutral template, *n*-dodecylamine. The inset in micrograph G is a single nanoparticle expanded to highlight the disordered mesopore structure.

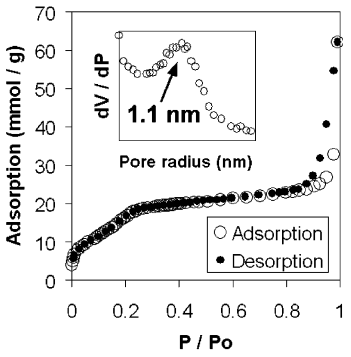

Figure 10. Liquid nitrogen adsorption isotherm of mesoporous silica nanoparticles of sample H using homogeneous conditions with neutral template. The inset shows the pore-radius distribution determined using the modified Kelvin equation.[18]

via any of these methods, and when precipitated they formed closely packed arrays. The inset of micrograph G is an expanded image of a single nanoparticle. In contrast to particles prepared using CTAB (A−F) disordered mesopores are clearly visible. A likely reason is that the shorter rod micelle lengths of templates in aprotic solvents[26] yield a higher frequency of defects during silicate deposition and formed a mesopore structure of lower symmetry. The particles also have spherical as opposed to faceted morphology. This is a clear example of nondirectional self-assembly and is consistent with the argument that a higher frequency of defects occur during particle growth. Disordered mesopore arrays are typical of materials prepared with a neutral template.[27]

Finally, the liquid nitrogen isotherm of sample H is shown in Figure 10, and as with all the samples, the isotherm is type IV in IUPAC classification and showed no hysteresis in the desorption branch of the first step. The adsorption capacity for sample H at 0.8 P/Po was 0.79 $cm^3\ g^{-1}$, comparable to 0.72 $cm^3\ g^{-1}$ as obtained by Büchel and co-workers.[9] A second hysteresis loop at high P/Po with a total adsorption of 2.2 $cm^3\ g^{-1}$ was assigned to adsorption between nanoparticles. Using the BET equation, a surface area of 1067 $m^2\ g^{-1}$ at STP was calculated. The pore radius distribution, with an average value of 1.1 nm calculated using the Kelvin equation, is shown in the inset.

The *n*-dodecylamine concentration for preparation of sample G (6.8×10^{-3} M) is significantly lower than the concentration of neutral template used by Grün and co-workers (2.2×10^{-2} M) in mesoporous particle synthesis and raises the question whether self-assembly of mesoporous materials using a neutral template is also silicate initiated.[29] Although there are several studies on the thermodynamics and mechanism of mesoporous silica growth using a charged template, there is very little information on synthesis using a neutral template. A charged template is assumed to interact with a silicate oligomer via very strong multidentate linkages. The resulting stable silica/surfactant molecules would have very low dissociation constants and subsequently very low critical micelle concentrations.[6] However, in the case of a neutral template, it is assumed that silicate oligomers interact with the template via much weaker hydrogen bonding.[27] Whether multidentate hydrogen bonding could lower the dissociation constant sufficiently to initiate self-assembly is something that has not been previously investigated. The observations of this work, showing that mesoporous nanoparticles still assemble at these very low concentrations is a strong indication that silicate-driven assembly is occurring, although our results cannot exclude the possibility that other factors, such as aggregative growth, are important in the mechanism of self-assembly.[30]

For each experimental group, the size of nanoparticles scaled approximately with concentration of TEOS and surfactant. We can use this relationship to suggest a model for the mechanism of growth of mesoporous nanoparticles. Assuming complete reaction, the scaling between particle size and concentration implies that the number of nucleation sites is fixed at an early stage. The actual number of micelles present in a synthesis would be proportional to the total concentration of surfactant molecules minus the critical micelle concentration. If micelle-initiated nucleation were the dominant mechanism, more nucleation sites would be expected, leading to more nanoparticles of a constant or similar size, rather than similar numbers of nanoparticles of increasing size, as was observed. We suggest that the synthesis is silica-driven and that the nucleating site for nanoparticle growth is either oligomeric or polymeric silica. It is likely that polymeric silica forms via conventional silica chemistry in which the rate-limiting step is the hydrolysis of TEOS.[31] This model was also suggested by Frasch and co-workers, who proposed that silica polymers formed prior to mesoporous surfactant/silica precipitation and that CTAB micelles simply act as reservoirs, supplying surfactant ions to the preformed silicate polymers.[28] The surfactant ions assemble at the polymer surface and bind forming primary particles, which could be a silica−CTAB cluster, spherical, or rod-shaped micelle.

(27) Tanev, P. T.; Pinnavaia, T. J. *Science* **1995**, *267*, 865.
(28) Frasch, J.; Lebeau, B.; Soulard, M.; Patarin, J.; Zana, R. *Langmuir* **2000**, *16*, 9049.
(29) Grün. M.; Büchel, C.; Kumar, D.; Schumacher, K.; Bidlingmaier, B.; Unger, K. K. *Stud. Surf. Sci. Catal.* **2000**, *128*, 155.
(30) Ocana, M.; Rodriguez-Clemente, R.; Serna, C. J. *Adv. Mater.* **1995**, *7*, 212.
(31) Van Blaaderen, A.; Van Geest, J.; Vrij, A. *J. Colloid Interface Sci.* **1991**, *142*, 1.

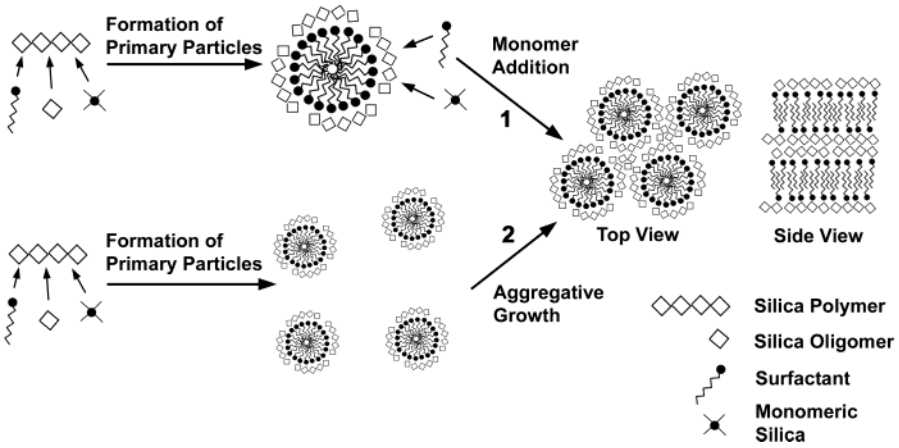

Figure 11. Scheme of the proposed mechanisms for the formation of ordered mesoporous silica nanoparticles in this study. In all cases silica polymers form initially via conventional silica chemistry.[38] The upper pathway corresponds to a monomeric silica addition mechanism referred to as mechanism 1 in the text. The lower pathway corresponds to mechanism 2, in which primary particles directionally aggregate to form particles with an ordered mesopore morphology. Nondirectional aggregative growth, mechanism 3 (not shown here) would proceed in a fashion similar to mechanism 2, but the final material would have a disordered mesopore structure.

The next phase of particle growth may occur via one or more of the following different mechanisms: (1) continued deposition of monomeric silica and surfactant ions onto existing primary particles; (2) directional aggregation where primary particles agglomerate together in an ordered fashion;[30] or (3) nondirectional aggregation where primary particles aggregate in a disordered fashion.[30] A cartoon to illustrate the various mechanisms possible is shown in Figure 11. A process similar to mechanism (1) is the formation of monodispersed microporous silica particles using the La Mer method where silica nucleation sites are coated with successive additions of monomeric silica at low concentrations.[32] Directional aggregation, mechanism (2), was first observed for the synthesis of elongated goethite (α−FeOOH) particles.[30,33] The nucleation step is the hydrolysis of ferric percolate to form primary particles approximately 3 nm in diameter. These particles then aggregate along a crystal axis giving uniform crystals approximately 100 nm long. Ordered nanoparticles prepared using the CTAB template could form via mechanism (2), where primary particles align along crystal planes, similar to the model proposed by Cai and co-workers in which silicate/surfactants rod-micelles form in the first step and then pack together in an ordered fashion to form mesoporous nanoparticles.[8] A synthesis that is thought to occur via nondirectional aggregation, mechanism (3), is the formation of highly monodispersed nanoparticles of microporous silica using the Stöber method.[23,31] In the Stöber method, primary particles of amorphous silica form in the first step and then these aggregate in a random fashion.[31] In this work, the synthesis of nanoparticles using a neutral template fits very well with a nondirectional aggregative growth process, where silica/surfactant clusters would bind together randomly and the final structure is highly monodispersed with disordered mesopores. It is conceivable that all nanoparticles prepared in this work could form via mechanism (1), however we cannot exclude the possibility that a combination of mechanisms would occur. To develop a definitive model for the mechanism of synthesis of mesoporous particles with controlled size, a more detailed investigation would be required in which each of the parameters is varied individually and their behavior during mesopore particle formation is studied using a variety of characterization techniques.

A final point regarding the work presented here is that we were also able to precipitate monodispersed mesoporous particles to form closely packed arrays. There is a great deal of interest in the assembly of spherical silica particles on surfaces, such as onto silicon wafers for the design of photonic crystals.[34] The main requirements for array formation is that the particles are uniform in size. The precipitation of mesoporous nanoparticles via our method may provide a new, convenient route for the construction of these materials. It may also be possible to control the precipitation of these spheres by functionalizing surfaces prior to precipitation using micropen lithography techniques.[35] Mesoporous spherical nanoparticles may also have applications in areas where monodispersed microporous silica particles are used.[36] An example of this is chemomechanical polishing of glass compositions for application in laser optics and mirrors where synthesis of monodispersed particles over a wide range of sizes is important for the manufacture of materials with specific polish grades.[36]

Conclusion

Mesoporous silica nanoparticles were prepared in a range of particle sizes from 65 to 740 nm by changing only the initial concentration of reactants. The smaller particles were stable in suspension for several days under quiescent conditions. Irregular as well as smooth spheres, with highly ordered mesoporous channels, were synthesized using charged template CTAB under het-

(32) La Mer, V. K.; Dinegar, R. H. *J. Am. Ceram. Soc.* **1950**, *72*, 4847.
(33) Murphy, P. J.; Posner, A. M.; Quirk, J. P. *J. Colloid. Interface Sci.* **1976**, *56*, 284.
(34) Ozin, G. A.; Yang, S. M. *Adv. Funct. Mater.* **2001**, *11*, 95.
(35) Fan, H.; Lu, Y.; Stump, A.; Reed, S. T.; Baer, T.; Schunk, R.; Perez-Luna, V.; Lopez, G. P.; Brinker, C. J. *Nature* **2000**, *405*, 56.
(36) Vacassey, R.; Flatt, R. J.; Hofmann, H.; Choi, K. S.; Singh, R. K. *J. Colloid Interface Sci.* **2000**, *227*, 302.

erogeneous and homogeneous conditions, respectively. For nanoparticles prepared under homogeneous conditions with a charged template a starburst mesopore structure could be obtained. Under homogeneous conditions and using a neutral template, *n*-dodecylamine, monodispersed regular spheres with disordered channels were obtained. The materials have high thermal stability, mesopore volumes ranging from 0.64 to 0.93 $cm^3\ g^{-1}$, and surface areas ranging from 917 to 1373 $m^2\ g^{-1}$. All samples exhibited two steps in their isotherms, with and without hysteresis corresponding to channel filling and adsorption between particles, respectively. We suggest that the mechanism of formation particles is driven by the formation of silica oligomers or polymers, and their relative stability in different solvent conditions determines the overall morphological arrangement of mesopores, which can change from parallel to starburst to disordered.

Acknowledgment. We thank Prof. Arvind Varma and Prof. Paul J. McGinn from the Department of Chemical Engineering, University of Notre Dame for use of the Quantachrome Autosorb-1 and the Scintag XDS 2000 diffractometer, respectively. The Radiation Laboratory is supported by the Office of Basic Energy Sciences, Division of Chemical Sciences, U.S. Department of Energy. This is contribution NDRL 4360 from the Radiation Laboratory.

CM0204371